15th Australasian Fluid Mechanics Conference
The University of Sydney, Sydney, Australia
13-17 December 2004

A Numerical Study of the Application of Radial Basis Function and Generalised Smoothed Particle Hydrodynamics to CFD

J. Ha

CSIRO Mathematical & Information Sciences
Clayton, VIC, 3168, AUSTRALIA

Abstract

Mesh free methods can be grouped into two approaches. One is based on field approximations such as moving least square approximations and radial basis functions (RBF) and the other is based on kernel approximations such as smoothed particle hydrodynamics (SPH). This paper presents an unified approach to implement the RBF and SPH methods for solving partial differential equations in general and for solving problems in computational fluid dynamics in particular.

There are many forms of RBF and SPH. This paper restricts attention to multiquadric and compactly supported RBFs and a particular SPH that satisfies certain completeness and reproducing conditions. Completeness and reproducing conditions enables SPH to incorporate boundary conditions in similar fashions to mesh based methods such as finite element. A number of numerical examples are presented to demonstrate the effectiveness of the two mesh free methods. Some remarks with respect to their computational efficiencies and implementation are also discussed.

Introduction

Mesh free methods have attracted much attention recently. Two distinct directions are followed by these methods. One is based on field approximations such as radial basis functions (RBF), element free Galerkin and moving least square approximations. The other is based on kernel approximations such as smoothed particle hydrodynamics.

The kernel approximations used in the original SPH proposed by Lucy [15] and Gingold and Monaghan [7] fail to reproduce linear functions. Various approaches to remedy these inaccuracies have been reported in the literature. It has been shown that the kernel approximations can be corrected so that they reproduce linear functions exactly (see, for example, Belytschko et al. [1]. Other workers, such as Johnson and Beissel [9], Randles and Libersky [19], and Krongauz and Belytschko [11], developed corrected derivative methods. Essentially, these methods replace the standard SPH interpolant with more sophisticated interpolant that was constructed by imposing the consistency conditions. Liu et al. [13] showed that the reproducing kernel provides boundary correction as well as removing the tensile instability. Chen and Beraun [3], on the other hand, developed a generalised SPH method (GSPH) by applying the kernel estimate into the Taylor series expansion. Their formulation extends not only the ability of standard SPH to model partial differential equations with higher order derivatives but to enforce boundary conditions directly as well.

In the last decade or so, another group of mesh free methods that is based on the function approximation by RBFs either globally or compactly supported was developed to solve partial differential equations (see, for example, Kansa [10]). RBF interpolation is required to be exact at the nodes, so one drawback of these methods is the need to solve the full coefficient matrix arising from the function approximation. A common approach to improve computational efficiency is to ensure sparsity, either by using functions of compact support, or by using domain decomposition (see, for example, Dubal [5]). In this paper, we applied the approach of SPH to RBF in using the nearest neighbours of a particle for estimating its derivatives. Thus, computer programs implementing the SPH and RBF methods can share the same structure. They differ only in their different estimates of the derivatives. The aim of this paper is to present the results of such implementation of RBF, and to compare them to GSPH. Most applications of standard SPH are to simulate compressible fluids. The second aim is to study the application of GSPH to two benchmark incompressible fluid problems for testing CFD codes. Also unlike standard SPH discretisation, all the numerical examples are obtained from substituting each term of the governing equations by their corresponding RBF or GSPH derivative approximations directly.

Generalised SPH

Applying the kernel approximation to the Taylor series expansion for $f(x)$ in the neighbourhood of x, Chen and Beraun [3] derived results that improve the approximation accuracy of SPH. In 1D, the GSPH approximation of a function $f(x)$ and its first two derivatives are given in Equations (1)-(3). Higher derivatives can easily be derived.

$$f(x) = \frac{\int f(x')W(x-x',h)dx'}{\int W(x-x',h)dx'} \tag{1}$$

$$\frac{df(x)}{dx} = \frac{\int (f(x)-f(x'))\frac{dW}{dx}dx'}{\int (x-x')\frac{dW}{dx}dx'} \tag{2}$$

$$\frac{d^2f(x)}{dx^2} = \frac{\int (f(x)-f(x'))\frac{d^2W}{dx^2}dx' - \frac{df}{dx}\int (x-x')\frac{d^2W}{dx^2}dx'}{0.5\int (x-x')^2\frac{d^2W}{dx^2}dx'} \tag{3}$$

The same procedure can be followed to derive approximations for functions in higher dimensions. However, the derivative estimates for higher dimensions involve matrix inversion. It is clear that GSPH is computationally more expensive to use than conventional SPH. The extra terms in the above approximations can be interpreted as corrections to the boundary deficiency in the conventional SPH. The results are equivalent to some of the results of Liu et al. [13] and Krongauz and Belytschko [11] obtained from imposing certain completeness and consistency conditions. The above approximations are algebraically correct for a function if it is constant, for its first derivative if it is constant or linear, and for its second derivative if it is constant, linear or quadratic.

It is well appreciated that SPH is closely related to the finite element method. The main difference between the two methods is that the SPH kernel approximation of a function does not satisfy the Kronecker delta property. It is thus not possible to impose essential boundary conditions in conventional SPH. The inclusion of $f(x)$ and df/dx in the above first and second derivative estimates enable the direct insertion of Dirichlet and Neumann boundary conditions, if they exist, in the GSPH method.

Radial Basis Functions

The development of RBFs into a mesh free method for solving partial differential equations arises from the recognition that a radial basis function interpolant can be smooth and accurate on any set of nodes in any dimension. The starting point is that the approximation of a function $f(\mathbf{x})$ for a set of distinct points $\mathbf{x}_i, i = 1, \ldots, N$ can be written as a linear combination of N RBFs.

$$f(\mathbf{x}) = \sum_{i=1}^{N} \alpha_i \phi(||\mathbf{x} - \mathbf{x}_i||) \tag{4}$$

where $\phi(||\mathbf{x} - \mathbf{x}_i||)$ denotes a positive definite RBF. The unknown coefficients α_i are to be determined from the system of equations formed by $f(\mathbf{x}_j), j = 1, \ldots, N$. Once they are determined, the m-th spatial derivatives of $f(\mathbf{x})$ are approximated by taking the m-th spatial derivatives of the RBFs.

$$\frac{\partial^m f}{\partial x^m} = \sum_{i=1}^{N} \alpha_i \frac{\partial^m \phi}{\partial x^m} \tag{5}$$

The application of Equations (4) and (5) provides the framework for the numerical solution of partial differential equations and their boundary conditions.

There are many RBFs either globally or compactly supported. An example of a globally supported RBF that is used extensively is multiquadric (MQ): $\phi(r) = (r^2 + c^2)^{1/2}$, where $r = ||\mathbf{x} - \mathbf{x}_i||$ and $c > 0$. It is well known that the shape parameter c strongly influences the accuracy of MQ approximation. An important unsolved problem is to find a method to determine the optimal value of c^2. To improve boundary treatment, methods using MQ usually have a polynomial of zero degree added to the right hand side of Equation 4.

The compactly supported RBFs are generally expressed in the form $\phi(r) = (1-r)_+^n p(r)$ (Wu [21] and Wendland [20]), and

$$(1-r)_+^n = \begin{cases} (1-r)^n & 0 \leq r < 1, \\ 0 & r \geq 1 \end{cases} \tag{6}$$

where $p(r)$ is a prescribed polynomial. By replacing r with r/δ for $\delta > 0$, the basis function has support on $[0, \delta]$. It is clear that the value δ defines the band width of the coefficient matrix. In general, the smaller the value of δ, the greater is the number of zero entries in the coefficient matrix resulting in lower accuracy. In the numerical results for compactly supported RBF, the Wendland function used is $\phi(r) = (1-r)^4(4r+1)$.

In this paper, we applied the approach of SPH to RBF in that only neighbouring particles within a given radial distance from the particle of interest are used in estimating the particle's derivatives. This has the advantage of avoiding the inversion of large coefficient matrix making problems requiring large number of nodes more amenable to numerical solution. In general, the larger the supporting region the higher is the accuracy of the approximation. The need to invert coefficient matrix makes the method more expensive than the generalised SPH.

Numerical Examples

First, the GSPH and RBF approximations of $\partial u/\partial x$ of the function $u(x,y) = \sin(\pi r) + \cos(2\pi r)$ are studied, where $r = \sqrt{x^2 + y^2 + 0.1}$. The L1-norms of error for a range of particle size and width of the supporting region are first computed to determine the optimal values of c^2 and δ to use for MQs RBF (MQRBF) and compactly supported RBF (CSRBF) respectively. Figure 1 compares the errors of GSPH with those of CSRBF and MQRBF using the optimal values of c^2 and δ obtained but different supporting regions ranging from $2h - 5h$, where h denotes the smoothing length. It shows that the RBF methods give better accuracy than the generalised SPH at the expense of more computational effort.

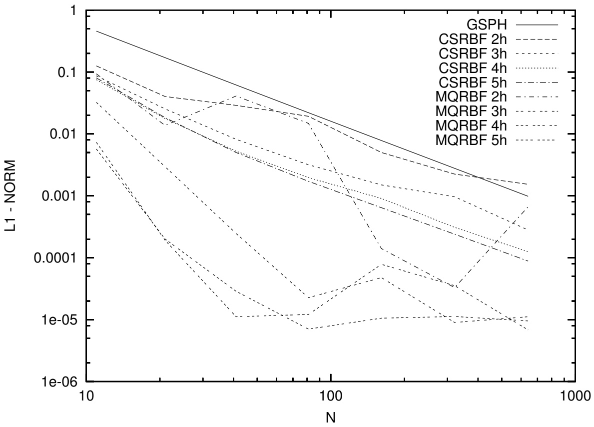

Figure 1: L1-norm errors for estimating $\partial u/\partial x$.

To demonstrate that the GSPH method can impose boundary conditions directly, the following heat conduction problem is solved in the domain $0 \leq x \leq 1$, $0 \leq y \leq 1$, initial condition $T(x,y,0) = -1$, Neumann boundary condition $\partial T(x,1,t)/\partial y = 0$ at $y = 1$ and Dirichlet condition at the other boundaries $T(0,y,t) = T(1,y,t) = T(x,0,t) = 1$.

$$\frac{\partial T}{\partial t} = \frac{\partial^2 T}{\partial x^2} + \frac{\partial^2 T}{\partial y^2} \tag{7}$$

where T denotes temperature and t time. Both RBF and GSPH give the result shown in Figure 2 and appear identical to the result obtained by Jeong et al. [8] who implement the boundary conditions to the conventional SPH in a different way.

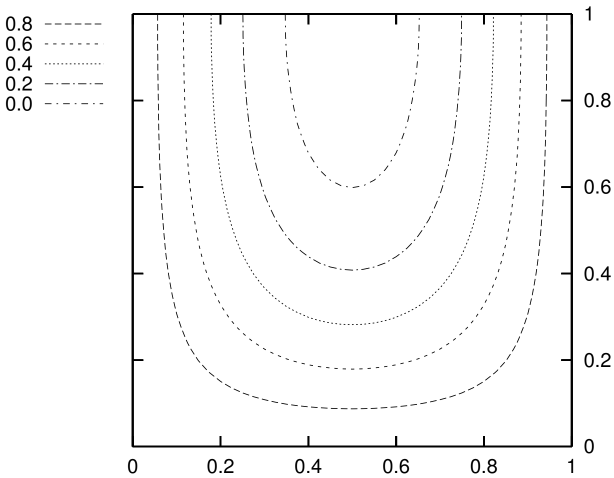

Figure 2: Temperature profiles at $t = 0.08$.

Next, the 3D Burger's equation is solved using GSPH and MQRBF and the numerical results are compared with the analytical solution.

$$\frac{\partial \mathbf{v}}{\partial t} + \mathbf{v} \cdot \nabla \mathbf{v} - \nu \nabla^2 \mathbf{v} = 0 \tag{8}$$

where $\mathbf{v}$ and ν denote velocity and viscosity respectively. The solution becomes more shock-like as the viscosity parameter decreases. Figure 3 compares L1-norm errors for GSPH and MQRBF for $\nu = 0.05$. The number of particles used is $41 \times 41 \times 41$. In general, MQRBF gives a slightly more accurate result than GSPH.

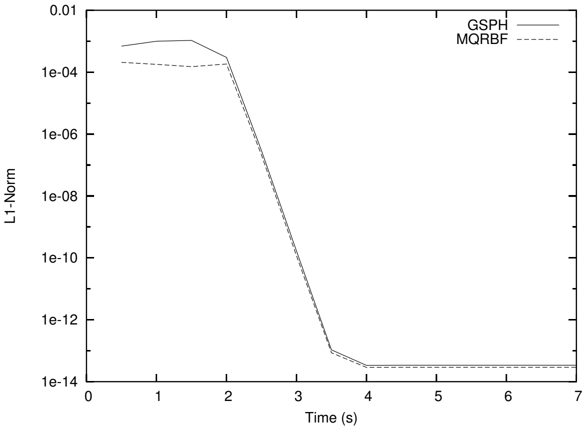

Figure 3: L1-norm errors for solving 3D Burger's equation.

To conclude this section, the GSPH method is applied to two standard CFD test problems - 2D lid-driven flow and natural convection in a square cavity. For the lid-driven cavity problem, the following Navier Stokes equation in 2D is solved

$$\frac{\partial \mathbf{v}}{\partial t} + \mathbf{v} \cdot \nabla \mathbf{v} + \frac{1}{\rho} \nabla p - \nu \nabla^2 \mathbf{v} = 0 \tag{9}$$

where p denotes pressure. The boundary conditions are $\mathbf{v} = (1,0)$ on $y = 1$ and $\mathbf{v} = (0,0)$ on the other three sides of the unit square. For an incompressible fluid, the Navier Stokes equation is complemented by the incompressibility constraint, $\nabla \cdot \mathbf{v} = 0$.

In general, velocity $\mathbf{v}^{n+1}$ at time t^{n+1} obtained by solving Equation (9) does not satisfy the incompressibility constraint. This constraint on velocity must be satisfied at all times. In this paper, the following steps are iterated until $\nabla \cdot \mathbf{v} \approx 0$ is reached.

1. $\Delta p_k^n = -\gamma \nabla \cdot \mathbf{v}_k^{n+1}$
2. $\Delta \mathbf{v}_k^{n+1} = \Delta t \nabla (\Delta p_k^n)$

Here, k is the iteration counter and $\Delta f_k = f_{k+1} - f_k$. Upon convergence, the above procedure gives the new pressure p^{n+1} and divergent free velocity $\mathbf{v}^{n+1}$ for time t^{n+1}. The parameter γ controls the rate of convergence and must satisfy the stability requirements $0 \le \gamma \le (\Delta x)^2/4\Delta t$. The iteration is equivalent to solving a Poisson equation for the pressure.

Figure 4 shows that the GSPH solutions for Reynolds number 1000 on a 129×129 grid using 3 different kernels compare well with the benchmark solutions 1 and 2 of Ghia et al. [6] and Botella and Peyret [2] respectively. In the figure, W3 denotes the cubic spline kernel of Monaghan [17], W4 the quartic spline kernel of Liu et al [14] and W5 the quintic spline kernel of Morris et al. [18]. For this problem, W4 gives the best result and W5 the worst result.

For incompressible fluid flow in a differentially heated square cavity of side L, the following equations are solved

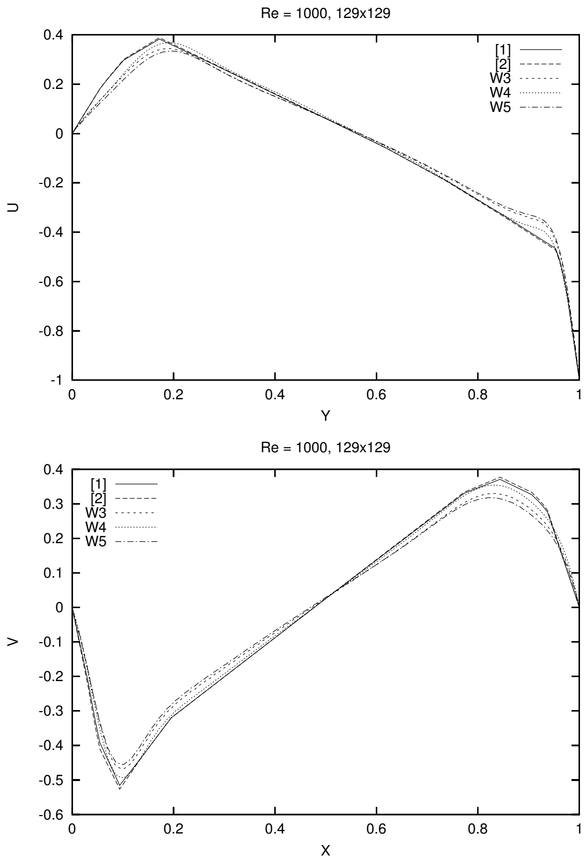

Figure 4: Comparison of lid-driven cavity results.

$$\frac{\partial \mathbf{v}}{\partial t} + \mathbf{v} \cdot \nabla \mathbf{v} + \frac{1}{\rho} \nabla p - \nu \nabla^2 \mathbf{v} = \beta (T - T_r) \mathbf{g} \tag{10}$$

$$\frac{\partial T}{\partial t} + \mathbf{v} \cdot \nabla T = \alpha \nabla^2 T \tag{11}$$

where α denotes thermal diffusivity, β the coefficient of thermal expansion and $\mathbf{g}$ the gravity. The initial conditions are $\mathbf{v}(x,y,0) = (0,0)$ and $T(x,y,0) = T_r$. The boundary conditions are $\mathbf{v} = (0,0)$ on cavity boundary, $T(0,y,t) = T_h$, $T(L,y,t) = T_c$, $\partial T(x,0,t)/\partial y = \partial T(x,L,t)/\partial y = 0$. Here, T_r, T_h and T_c denote the reference, hot and cold wall temperatures respectively. Table 1 shows that the GSPH results compares well with the benchmark solutions for Prandtl number 0.71 and Rayleigh numbers 10^4 - 10^6. In the table, the numbers enclosed by [] and () are the results of Leal et al. [12] and de Vahl Davis [4] respectively.

	$\bar{u}_{max}$	$\bar{y}$	$\bar{v}_{max}$	$\bar{x}$
	[16.18]	[0.823]	[19.63]	[0.119]
Ra = 10^4	16.18	0.822	19.63	0.119
	(16.178)	(0.823)	(19.617)	(0.119)
	[34.74]	[0.855]	[68.62]	[0.066]
Ra = 10^5	34.76	0.853	68.64	0.0656
	(34.73)	(0.855)	(68.59)	(0.066)
	[64.83]	[0.850]	[220.6]	[0.0379]
Ra = 10^6	64.91	0.847	220.72	0.0375
	(64.63)	(0.850)	(219.36)	(0.0379)

Table 1: Comparison of natural convection results.

Even for unsteady problems, the pseudo-compressibility formulation may also be used above to enforce the incompressibility condition provided that some relations between the relevant parameters hold (Mendez and Velazquez [16]). In this method, the pseudo-compressibility equation $\partial p/\partial\tau = -c\nabla\cdot\mathbf{v}$ is solved together with equation (9) or equations (10) and (11), where c is the pseudo-compressibility coefficient. For Reynolds numbers in the range of 100-1000, c values of 100 give accurate solutions. When steady solutions are sought, c values of 5-10 can be used. The pseudo-compressibility method gives almost identical results to the above two test problems and is computationally less expensive than solving the Poisson equation for pressure.

Conclusions

This paper presents an unified approach to implement the RBF and SPH methods for numerical computations. The approach of SPH in using the nearest neighbours within the supporting region of a particle to estimate its derivatives of a function is applied to RBF. The size of supporting region depends on the smoothing kernel used in the case of SPH but is a parameter in the case of RBF. In the numerical examples considered in this paper, a supporting region of width $3h$ for RBF gives accurate results provided that optimal values for the parameters c^2 and δ are used. There are attempts reported in the literature but it is still an important unsolved problem of how to determine the optimal value for these parameters.

The numerical examples presented in the last section demonstrated that GSPH and RBF give accurate results to the problems considered. Unlike conventional SPH, they have the advantage of being able to impose boundary conditions directly. Also, they are just as easy to implement as the conventional SPH. There is no dimensional difference between 1D, 2D and 3D as far as computer coding for their implementation is concerned. Apart from correcting the boundary deficiency problem, GSPH is less affected by particle disorder than conventional SPH because of the normalisation term in the denominator (refer to Equations 1-3).

Acknowledgements

The author thanks Dr N. Stokes of CSIRO Mathematical and Information Sciences for valuable discussions.

References

[1] Belytschko, T., Krongauz, Y., Organ, D., Fleming, M. and Krysl, P., Meshless methods: An overview and recent developments, *Comput. Meth. Appl. Mech. Engng.*, **139**, 1996, 3-47.

[2] Botella, O. and Peyret, R., 1998. Benchmark spectral results on the lid-driven cavity flow, *Computers & Fluids*, **27**, 421-433.

[3] Chen, J.K. and Beraun, J.E., A generalized smoothed particle hydrodynamics method for nonlinear dynamic problems, *Comput. Methods Appl. Mech. Engrg.*, **190**, 2000, 225-239.

[4] de Vahl Davis, G., Natural convection of air in a square cavity: a benchmark numerical solution, *Int. J. Numer. Methods Fluids*, **3**, 1983, 243-264.

[5] Dubal, M.R., Domain decomposition and local refinement for multiquadric approximations. I: Second-order equations in one-dimension, *Int. J. Appl. Sci. Comput.*, **1**, 1994, 146-171.

[6] Ghia, U., Ghia, K.N. and Shin, C.T., High-Re solutions of incompressible flow using the Navier-Stokes equations and a multigrid method, *Journal of Computational Physics*, **48**, 1982, 387-411.

[7] Gingold, R. and Monaghan, J., Smoothed particle hydrodynamics: theory and application to non-spherical stars, *Mon. Not. Roy. Astron. Soc.*, **181**, 1977, 375-389.

[8] Jeong, J.H., Jhon, M.S., Halow, J.S. and van Osdol, J., Smoothed particle hydrodynamics: Applications to heat conduction, *Computer Physics Communications*, **153**, 2003, 71-84.

[9] Johnson, G.R. and Beissel, S.R., Normalized smoothing functions for SPH impact calculations, *Int. J. Numer. Meth. Engng.*, **39**, 1996, 2725-2741.

[10] Kansa, E.J., Multiquadrics - A scattered data approximation scheme with applications to computational dynamics - I. Surface approximations and partial derivative estimates, *Comput. Math. Appl.*, **19**, 1990, 127-145.

[11] Krongauz, Y. and Belytschko, T., Consistent pseudo-derivatives in meshless methods, *Comput. Meth. Appl. Mech. Engng.*, **146**, 1998, 371-386.

[12] Leal, M.A., Perez-Guerrero, J.S. and Cotta, R.M., Natural convection inside two-dimensional cavities: the integral transform method, *Communications i n Numerical Methods in Engineering*, **15**, 1999, 113-125.

[13] Liu, W.K., Jun, S., Adee, J. and Belytschko, T., Reproducing kernel particle methods for structural dynamics, *Int. J. Numer. Meth. Engng.*, **38**, 1995, 1655-1679.

[14] Liu, M.B., Liu, G.R. and Lam, K.Y., Constructing smoothing functions in smoothed particle hydrodynamics with applications, *Journal of Computational a nd Applied Mathematics*, **155**, 2003, 263-284.

[15] Lucy, L.B., A numerical approach to the testing of the fission hypothesis, *J. Astron.*, **82**, 1977, 1013-1024.

[16] Mendez, B. and Velazquez, A., Finite point solver for the simulation of 2-D laminar incompressible unsteady flows, *Computer Methods in Applied Mechanics and Engineering*, **193**, 2004, 825-848.

[17] Monaghan, J.J., Smoothed particle hydrodynamics, *Ann. Rev. Astron. Astrophys.*, **30**, 1992, 543-574.

[18] Morris, J.P., Fox, P.J. and Zhu, Y., 1997. Modeling low Reynolds number incompressible flows using SPH, *J. Comput. Phys.*, **136**, 214-226.

[19] Randles, P.W. and Libersky, L.D., Smoothed particle hydrodynamics: some recent improvement and applications, *Comput. Methods Appl. Mech. Eng.*, **139**, 1996, 375-408.

[20] Wendland, H., Piecewise polynomial, positive definite and compactly supported radial functions of minimal degree, *Adv. Comput. Math.*, **4**, 1995, 389-396.

[21] Wu, Z., Compactly supported positive definite radial functions, *Adv. Comput. Math.*, **4**, 1995, 283-292.